# α-Solanine inhibits growth and metastatic potential of human colorectal cancer cells

XIA YAN[1,2], MIAO LI[1,2], LEI CHEN[1,2], XIAO PENG[1,2], ZU-JUN QUE[1],
HONG-MEI AN[3], KE-PING SHEN[2] and BING HU[1,2]

[1]Institute of Traditional Chinese Medicine in Oncology; [2]Department of Oncology; [3]Department of Science and Technology,
Longhua Hospital Shanghai University of Traditional Chinese Medicine, Shanghai 200032, P.R. China

**Abstract.** *Solanum nigrum* L. (Longkui) is one the most widely used anticancer herbs in traditional Chinese medicine. α-Solanine is an important ingredient of *S. nigrum* L. and has demonstrated anticancer properties in various types of cancer. However, the effects of α-solanine on colorectal cancer remain elusive. The aim of the present study was to assess the effects of α-solanine on human colorectal cancer cells. The results demonstrated that α-solanine inhibited the proliferation of RKO cells in a dose- and time-dependent manner. In addition, α-solanine arrested the cell cycle at the G0/G1 phase and suppressed the expression levels of cyclin D1 and cyclin-dependent kinase 2 in RKO cells. α-Solanine induced apoptosis of RKO cells, as indicated by morphological changes and positive Annexin-FITC/propidium iodide staining. Additionally, α-solanine activated caspase-3, -8 and -9 in RKO cells, which contributed to α-solanine-induced apoptosis. α-Solanine also increased the generation of reactive oxygen species, which contributed to caspase activation and induction of apoptosis. α-Solanine inhibited the migration, invasion and adhesion of RKO cells, as well as the expression levels and activity of matrix metalloproteinase (MMP)-2 and MMP-9. In addition, α-solanine inhibited cell proliferation, activated caspase-3, -8 and -9, induced apoptosis, and inhibited the migration and invasion of HCT-116 cells. Furthermore, α-solanine inhibited tumor growth and induced apoptosis *in vivo*. These findings demonstrated that α-solanine effectively suppressed the growth and metastatic potential of human colorectal cancer.

*Correspondence to:* Dr Bing Hu, Institute of Traditional Chinese Medicine in Oncology, Longhua Hospital Shanghai University of Traditional Chinese Medicine, 725 South Wanping Road, Shanghai 200032, P.R. China
E-mail: beearhu@hotmail.com; beearhu@shutcm.edu.cn

Professor Ke-Ping Shen, Department of Oncology, Longhua Hospital Shanghai University of Traditional Chinese Medicine, 725 South Wanping Road, Shanghai 200032, P.R. China
E-mail: shen0313@163.com

## Introduction

Colorectal cancer is the third most common malignant tumor and the second leading cause of cancer-related mortality worldwide (1). The currently available therapeutic options for colorectal cancer include surgery, chemotherapy and targeted therapy (2). Surgery has been reported to be highly effective for colorectal cancer, although some patients develop metastasis postoperatively (3). Chemotherapy, including 5-fluorouracil, capecitabine, oxaliplatin and irinotecan, is also used for colorectal cancer, but it may be accompanied by major side effects, such as neutropenia, nausea, vomiting and hepatorenal toxicity, and its efficacy has been reported to be relatively unsatisfactory (4). Targeted therapies for colorectal cancer have recently been introduced, mainly involving epidermal growth factor receptor, angiogenesis and immune checkpoint targeting; however, a satisfactory effect was only achieved in a small number of patients (5-7). Therefore, developing new therapeutic approaches to colorectal cancer is crucial.

Traditional Chinese medicine (TCM) is a major biomedical resource. TCM has a long history in the treatment of colorectal cancer, as well as being a promising complementary and alternative therapy. TCM has been used in various treatment strategies for colorectal cancer to date, aimed at inhibiting tumor growth, reducing side effects, enhancing the therapeutic effects of chemotherapy, improving the quality of life, regulating immune function, and prolonging patient survival (8,9). *Solanum nigrum* L. (Longkui) is one of the most commonly used anticancer Chinese herbs in clinical practice, and it has been confirmed to have important anticancer properties (10).

In colorectal cancer, *S. nigrum* L. was found ti inhibit cell proliferation, induce autophagy, enhance the therapeutic effect of chemotherapy, and inhibit cell adhesion, migration and invasion (11,12).

α-Solanine is one of the main components of *S. nigrum* L, and it has been shown to exert anticancer effects on various types of cancer cells: It can inhibit proliferation, induce apoptosis and inhibit angiogenesis in breast cancer (13); it also inhibited the proliferation, migration and invasion of pancreatic cancer cells and suppressed tumor growth (14); in addition, α-solanine was shown to inhibit the invasion of prostate cancer cells by inhibiting epithelial-to-mesenchymal transition and lowering the expression levels of matrix metalloproteinases (MMPs) (15); furthermore, it promoted apoptosis of hepatocellular carcinoma cells by enhancing the generation of reactive oxygen species (ROS), accompanied by an increase in the expression levels of apoptosis signal-regulating kinase 1 and thioredoxin-binding protein-2 and a decrease in histone deacetylase 1 expression (16). The aim of the present study was to investigate the effects of α-solanine on human colorectal cancer cells.

## Materials and methods

*Chemicals and reagents*. RPMI-1640 medium, fetal bovine serum (FBS) and trypsin were purchased from Gibco; Thermo Fisher Scientific, Inc. The Cell Counting Kit-8 (CCK-8) was provided by Dojindo Co., Ltd. The Hoechst 33258 staining kit, caspase activity assay kit, ROS assay kit, Z-VAD-FMK, 2',7'-dichlorodihydrofluorescein diacetate (DCFH-DA) and N-acetyl-L-cysteine (NAC), were purchased from Beyotime Institute of Biotechnology. Antibodies against cyclin D1 (CCND1; cat no. BS1741), cyclin-dependent kinase (CDK)4 (cat no. MB0027), MMP-2 (cat no. BS1236), MMP-9 (cat. no. bs1241) and glyceraldehyde 3-phosphate dehydrogenase (GAPDH; cat no. AP0063) were purchased from Bioworld Technology, Inc. The Cell cycle and FITC Annexin V Apoptosis Detection kits were obtained from BD Pharmingen; BD Biosciences. The CytoSelect™ 48-Well Cell Adhesion Assay and CytoSelect™ 24-Well Cell Invasion Assay kits were manufactured by Cell Biolabs, Inc. α-Solanine was purchased from Santa Cruz Biotechnology, Inc. (CAS no. 20562-02-1, cat no. sc-252340, lot no. E1619) and its purity (as assessed by high-performance liquid chromatography) was >95%. The chemical structure of α-solanine is shown in Fig. 1. α-Solanine (10 mM) was dissolved in dimethyl sulfoxide (DMSO) and the same volume of DMSO was used as control.

*Cell culture*. Human colorectal cancer RKO and HCT-116 cells were obtained from and authenticated with short-tandem repeat analysis by The Cell Bank of Type Culture Collection of Chinese Academy of Sciences. The cells were cultured in RPMI-1640 medium with 10% FBS and 1% streptomycin-penicillin, and maintained at 37°C in a humidified atmosphere containing 5% $CO_2$.

*Cell proliferation assay*. In this study, $1x10^4$ colorectal cancer cells were inoculated into 96-well plates, and different concentrations of α-solanine with the same volume of DMSO were added after 24 h; an equal volume of DMSO was used as control. At different time points during treatment, 10 $\mu$l CCK-8 solution was added to the wells and incubated at 37°C for 2 h, and the optical density (OD) was measured by a plate reader (SpectraMax M5; Molecular Devices LLC) at the read mode of absorbance (450 nm). The cell survival rate was calculated as follows: Cell survival rate (%)=(experimental OD value/control OD value) x100%. The $IC_{50}$ of α-solanine was calculated using IBM® SPSS® Statistics 25 (IBM Corp.).

*Cell cycle detection*. RKO cells ($3x10^5$) were inoculated in 6-well plates. At 24 h after inoculation, the cells were treated with 0-25 $\mu$M α-solanine (final concentration) with the same volume of DMSO. After 48 h of treatment, the cells were collected, in with 75% ethanol, washed with phosphate-buffered saline (PBS), stained with 400 $\mu$l propidium iodide (PI) solution in the dark at room temperature for 15 min, and the cell cycle distribution was detected by flow cytometry.

*Hoechst 33258 staining*. A total of $5x10^3$ colorectal cancer cells were inoculated into 24-well plates and treated with different doses of α-solanine with the same volume of DMSO after 24 h of adherence. After 48 h of treatment, the cells were fixed by the fixative solution provided with the kit according to the manufacturer's instructions, stained by Hoechst 33258 for 20 min at room temperature in the dark, washed with PBS, and the cell morphology was observed under a fluorescence microscope (magnification, x200).

*Apoptosis detection*. Apoptosis was detected according to the manufacturer's instructions. Briefly, $3x10^5$ colorectal cancer cells were inoculated into 6-well plates and treated with different concentrations of α-solanine with the same volume of DMSO after 24 h of adherence. After 48 h of treatment, the cells were harvested, washed with PBS, resuspended in binding buffer, labeled by Annexin V-FITC, incubated with PI, and apoptosis was detected by flow cytometry.

*Caspase activity assay*. Caspase activity was detected according to the manufacturer's protocol. In brief, colorectal cancer cells were treated with different doses of α-solanine with the same volume of DMSO for 48 h, collected, lysed and quantified. The activities of caspase-3, -8 and -9 were detected using Ac-DEVD-pNA, Ac-IETD-pNA, and Ac-LEHD-pNA as substrates, respectively. For inhibition of caspases, RKO cells were pre-incubated with Z-VAD-FMK (100 $\mu$M) for 2 h, and then treated with different concentrations of α-solanine for 48 h.

*ROS assay*. RKO cells ($3x10^5$) were inoculated into 6-well plates and, after 24 h of adherence, the cells were treated with 0-25 $\mu$M α-solanine (final concentration) with the same volume of DMSO. After 48 h of treatment, the cells were stained with 1 ml DCFH-DA (1:1,000) at 37°C for 20 min and washed with serum-free RPMI-1640 medium. A fluorescence microscope was utilized for visualization, and fluorescence was detected by a plate reader (excitation wavelength at 488 nm and emission wavelength at 525 nm). For ROS inhibition, RKO cells were incubated with NAC (250 $\mu$M) for 2 h, and were then treated with different concentrations of α-solanine for 48 h.
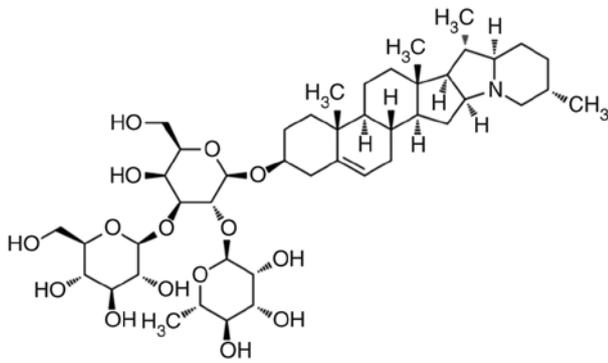
Figure 1. Chemical structure of α-solanine.

*Cell adhesion assay.* Cell adhesion was measured according to the manufacturer's protocol. Briefly, $5\times10^5$ RKO cells were inoculated into 6-well plates and treated with 0-12 $\mu$M α-solanine (final concentration) with same volume of DMSO. After 48 h of treatment, cells were collected and inoculated in extracellular matrix (ECM) pre-coated 24-well plates ($1.5\times10^5$), and cultured for 90 min. The cells were stained with Cell Stain Solution for 10 min at room temperature, and extracted with Extraction Solution for 10 min on an orbital shaker. The OD values (560 nm) of the wells were detected by a plate reader.

*Cell migration assay.* Cell migration was measured using the scratch assay (17,18). Briefly, $8\times10^5$ serum-starved colorectal cancer cells were inoculated into 6-well plates and cultured until the cell confluence was >95%. The cell layer was scratched on the bottom of the well with a sterile 20-$\mu$l pipette tip, washed with PBS, fresh culture medium was added, and the cells were treated with different doses of α-solanine with the same volume of DMSO for 48 h. Cell migration to the center of the scratch was observed under a phase-contrast microscope (magnification, x50) and measured by Adobe Photoshop CC 2014.

*Cell invasion assay.* The cell invasion assay was performed according to the manufacturer's instructions. Briefly, $3\times10^5$ colorectal cancer cells were added into the inner side of the insert and different doses of α-solanine with the same volume of DMSO was added to the wells. In addition, 500 $\mu$l RPMI-1640 supplemented with 10% FBS was added to the lower well of the invasion plate. After 48 h of treatment, the invading cells were stained with Cell Stain Solution for 10 min at room temperature, washed with PBS, and observed under a phase-contrast microscope (magnification, x200). For quantification, the invading cells were extracted with the Extraction Solution provided by manufacturer for 10 min on an orbital shaker and measured at an OD value of 560 nm by a plate reader.

*Western blot analysis.* Western blot analysis was performed as described previously (19,20). In brief, RKO cells were treated with 0-25 $\mu$M α-solanine (final concentration) with the same volume of DMSO for 48 h, collected, lysed with RIPA buffer (Beyotime Institute of Biotechnology), quantified by BCA Protein Assay Kit (Beyotime Institute of Biotechnology), and

subjected to 8-10% SDS-PAGE. The proteins (40 $\mu$g/lane) were transferred onto PVDF membranes. The membranes were then blocked with 5% non-fat milk for 2 h at room temperature, probed with antibodies against CNCD1 (1:1,000), CDK4 (1:1,000), MMP-2 (1:1,000), MMP-9 (1:1,000) and GAPDH (1:1,000) at 4˚C overnight and washed with PBST (0.1% Tween-20). The blots were then incubated with horseradish peroxidase (HRP)-conjugated secondary antibodies and visualized by an enhanced chemiluminescence substrate (Thermo Fisher Scientific, Inc.).

*Gelatin zymography assay.* The activities of MMP-2 and MMP-9 were determined by gelatin zymography. Briefly, α-solanine-treated cell culture supernatant was collected, quantified, and subjected to 10% SDS-PAGE containing 1 mg/ml gelatin without prior denaturation. The gels were washed with 2.5% Triton X-100 for 2 h at room temperature to remove SDS, washed with ddH$_2$O, incubated with developing buffer overnight at 37˚C, stained with Coomassie brilliant blue for 3 h at room temperature and de-stained in methanol/acetic acid. The activities of MMP-2 and MMP-9 were detected as unstained bands against a blue background.

*Animal model.* A total of 10 male 6-7-week-old BALB/c nude mice were purchased from the Shanghai SLAC Laboratory Animal Co.,Ltd. The mice were acclimatized for 1 week under pathogen-free conditions at the animal laboratory of Longhua Hospital with a 12-h light/dark cycle, regulated temperature of 24±2˚C and humidity of 50±10%, with *ad libitum* access to water and animal chow. The mice were injected with $2\times10^6$ RKO cells in 0.1 ml PBS in the right flank. When the tumors were palpable, the mice were randomly divided into two groups (5 mice/group) that did or did not receive 5 mg/kg α-solanine once per day. The tumor length (L) and width (W) were measured every 2 days by calipers and the tumor volume (Tv) was calculated according to the formula: $Tv=\pi/6 \times L \times W^2$. After 12 days of treatment (the diameter of the largest tumor was 17.68 mm), the mice were sacrificed under anesthesia and the tumors were removed, weighed and subjected to further experiments. All studies involving mice were approved by the Longhua Hospital Animal Care and Use Committee.

*TUNEL assay.* Apoptotic cells in tumor tissue were identified by TUNEL assay following the instructions of the manufacturer (Roche Diagnostics). The slides were examined under an Olympus light microscope (Olympus Corporation). Three fields at a magnification of x200 were randomly selected from each slide and apoptotic cells were counted by Image-Pro Plus 6.0 software (Media Cybernetics, Inc.).

*Immunohistochemistry.* The tumor tissues were fixed, embedded in paraffin, cut into 4-$\mu$m sections, blocked with 3% hydrogen peroxide, probed with Ki-67 antibody (1:100) at 4˚C overnight, followed by incubation with HRP-conjugated anti-rabbit/anti-mouse IgG secondary antibody (1:4,000) at 37˚C for 30 min and visualized using 3,3-diaminobenzidine at room temperature for 3 min. The sections were then counterstained with hematoxylin for 45 sec at room temperature and mounted with glass coverslips. The slides were examined under an Olympus light microscope (Olympus Corporation).
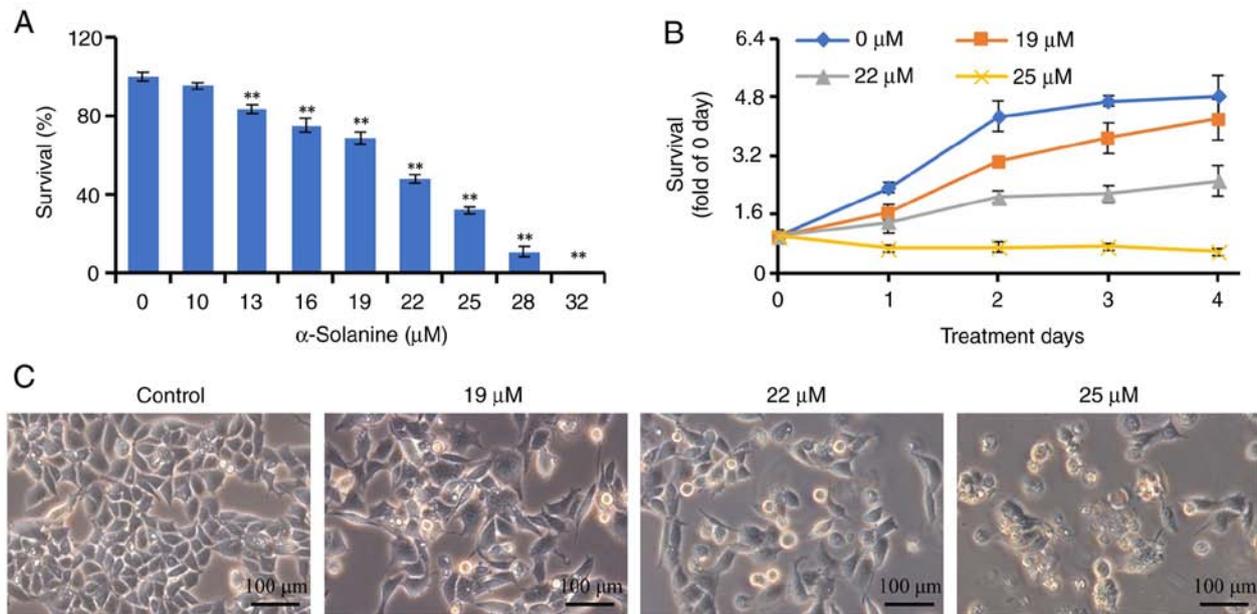
Figure 2. Effects of α-solanine on the growth of RKO cells. (A) RKO cells were treated with 10-32 $\mu$M α-solanine for 48 h and subjected to Cell Counting Kit-8 (CCK-8) assay. (B) RKO cells were treated with 19-25 $\mu$M α-solanine for 1-4 days and subjected to CCK-8 assay. (C) RKO cells were treated with 19-25 $\mu$M α-solanine for 48 h and observed under a microscope (magnification, x200). **P<0.01 vs. control group.

Three fields at a magnification of x200 were randomly selected from each slide and analyzed by Image-Pro Plus 6.0 software (Media Cybernetics, Inc.).

*Statistical analysis*. Data are expressed as mean ± standard deviation, and were analyzed by one-way analysis of variance and Dunnett's, Student-Newman-Keuls or least significance difference test. P<0.05 was considered to indicate statistically significant differences.

## Results

*α-Solanine inhibits the proliferation of RKO cells*. We first investigated the effects of α-solanine on cell growth. As shown in Fig. 2, 13-32 $\mu$M α-solanine significantly inhibited the proliferation of RKO cells in a dose-dependent manner, and the proliferation of RKO cells was fully inhibited following treatment with 32 $\mu$M α-solanine for 72 h (P<0.01). The IC$_{50}$ of α-solanine was 20.84 $\mu$M. Furthermore, 19-25 $\mu$M α-solanine inhibited the proliferation of RKO cells in both a dose- and time-dependent manner (P<0.05). Following treatment with α-solanine, the RKO cells became larger, exhibited a lower confluence, and 7.03, 12.52 and 29.78% of the cells died and floated in the 19, 22 and 25 $\mu$M groups, respectively.

*α-Solanine causes G0/G1 cell cycle arrest*. In the present study, the effects of α-solanine on the cell cycle distribution of RKO cells were examined by flow cytometry. As displayed in Fig. 3, treatment with α-solanine increased the number of RKO cells in the G0/G1 phase and decreased the number of RKO cells in the S phase and G2/M phase in a dose-dependent manner (P<0.01), indicating that α-solanine caused cell cycle arrest in the G0/G1 phase. Furthermore, the results of western blotting revealed that 19-25 $\mu$M α-solanine inhibited the expression levels of CCND1 and CDK4 in a dose-dependent manner.

*α-Solanine induces apoptosis of RKO cells*. The effects of α-solanine on apoptosis were investigated. Hoechst 33258 staining revealed that, after treatment with α-solanine, the number of RKO cells was decreased, and their distribution was sparse. In addition, the nuclei of some cells were densely stained or fragmented (9.81, 17.43 and 24.17% of the cells in the 19, 22 and 25 $\mu$M groups, respectively), indicating the occurrence of apoptosis. Furthermore, Annexin V-FITC/PI labeling and flow cytometry demonstrated that α-solanine at 19-25 $\mu$M promoted apoptosis of RKO cells in a dose-dependent manner (P<0.01; Fig. 4).

Apoptosis is a caspase-mediated programmed cell death (21). The effects of α-solanine on caspase activity were detected by an enzyme-substrate system. The results indicated that the activities of caspase-3, -8 and -9 were significantly increased following treatment with α-solanine (P<0.01). Z-VAD-FMK, a caspase inhibitor, was able to antagonize the effects of α-solanine on of RKO cell apoptosis (P<0.05), which suggested that caspases contributed to α-solanine-induced apoptosis (Fig. 4).

*α-Solanine induces ROS production in RKO cells*. High levels of ROS could promote apoptosis of tumor cells (22). It has been reported that α-solanine could induce the production of ROS in hepatocellular carcinoma cells (16). In the present study, ROS levels were detected by DCFH-DA staining. The findings demonstrated that, following treatment with α-solanine, the number of RKO cells emitting green fluorescence was increased, and the fluorescence density was markedly increased in a dose-dependent manner (P<0.01), indicating that α-solanine increased the ROS level in RKO cells. In addition, NAC, as a ROS scavenger, antagonized the effects of α-solanine on caspase-3, -8 and -9 (P<0.05) and apoptosis (P<0.01), suggesting that ROS contributed to α-solanine-induced activation of caspase-3, -8 and -9 and promoted apoptosis of RKO cells (Fig. 5).
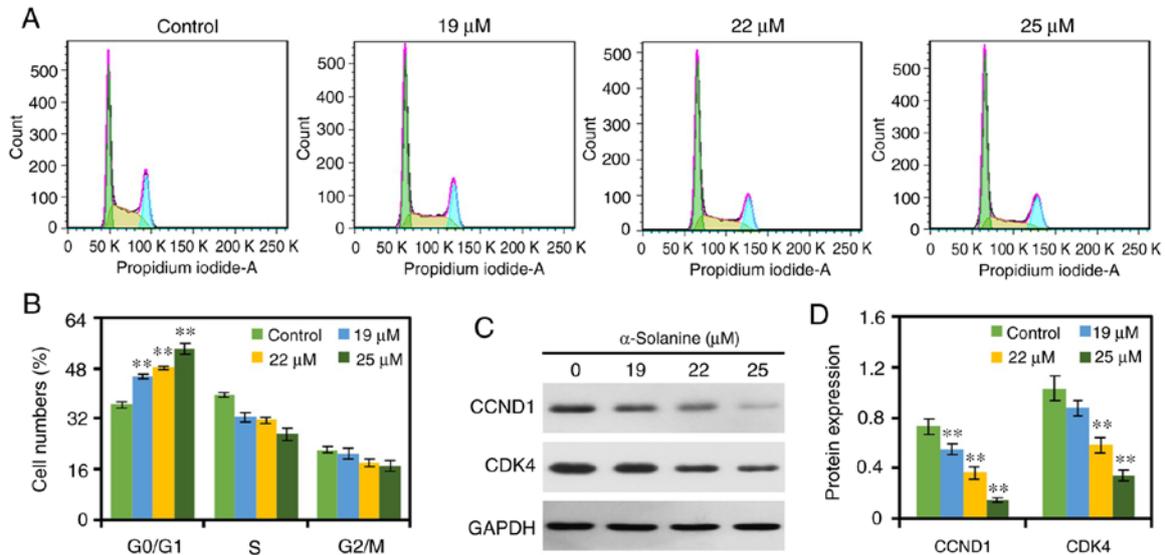
Figure 3. α-Solanine arrests the cell cycle of RKO cells. (A) RKO cells were treated with α-solanine and the cell cycle distribution was evaluated using flow cytometry, and (B) data were expressed as mean ± standard deviation. The expression levels of CCND1 and CDK4 were (C) detected by western blotting and (D) quantified by Quantity One. **P<0.01 vs. control group. CCND1, cyclin D1; CDK4, cyclin-dependent kinase 4.
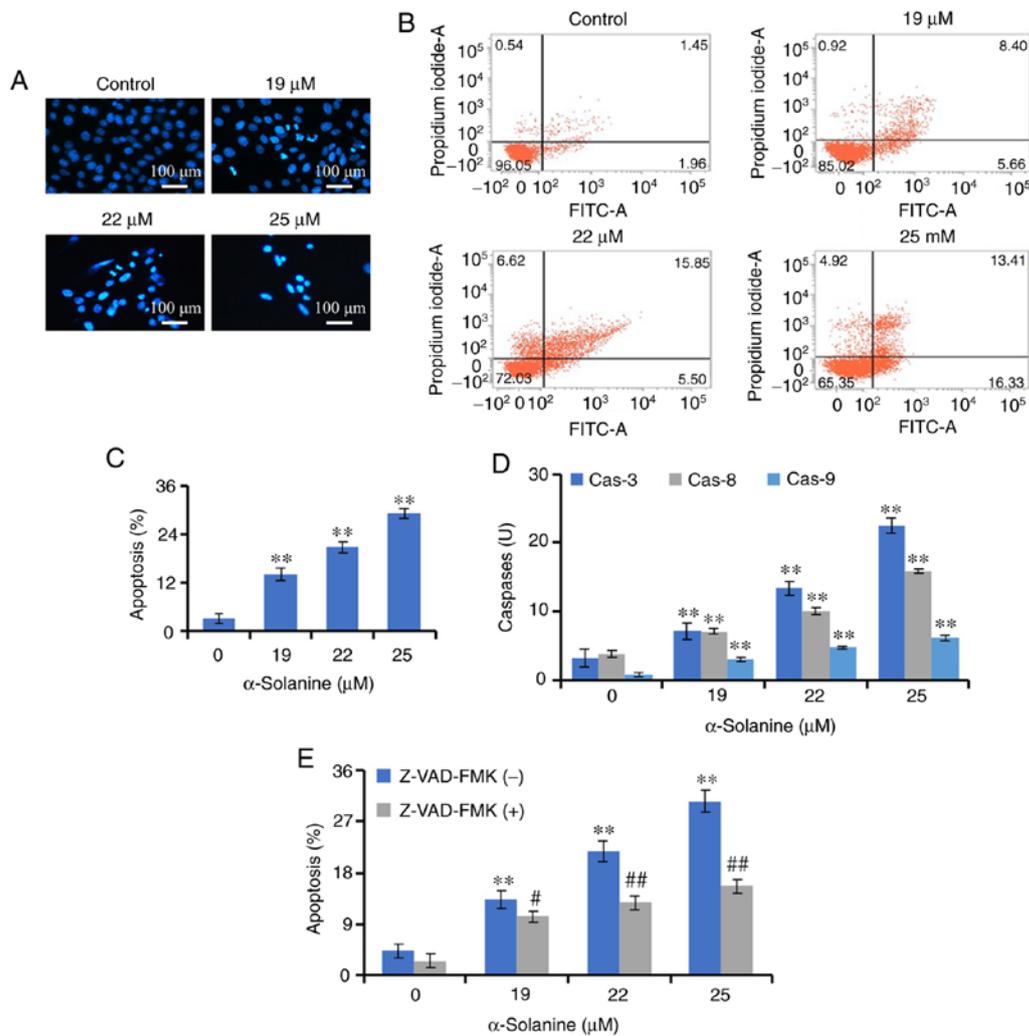


Figure 4. α-Solanine induces apoptosis in RKO cells. (A) RKO cells were treated with α-solanine, stained with Hoechst 33258, and observed under a microscope (magnification, x200). (B) α-Solanine-treated RKO cells were subjected to AnnexinV-FITC/PI staining, analyzed by flow cytometry and (C) the results were expressed as mean ± standard deviation. (D) The activities of caspase-3, -8 and -9 were detected in α-Solanine-treated RKO cells. (E) RKO cells were pre-treated with Z-VAD-FMK, subjected to α-solanine treatment, and apoptosis was detected. **P<0.01 vs. control group; #P<0.05, ##P<0.01 vs. α-solanine group.
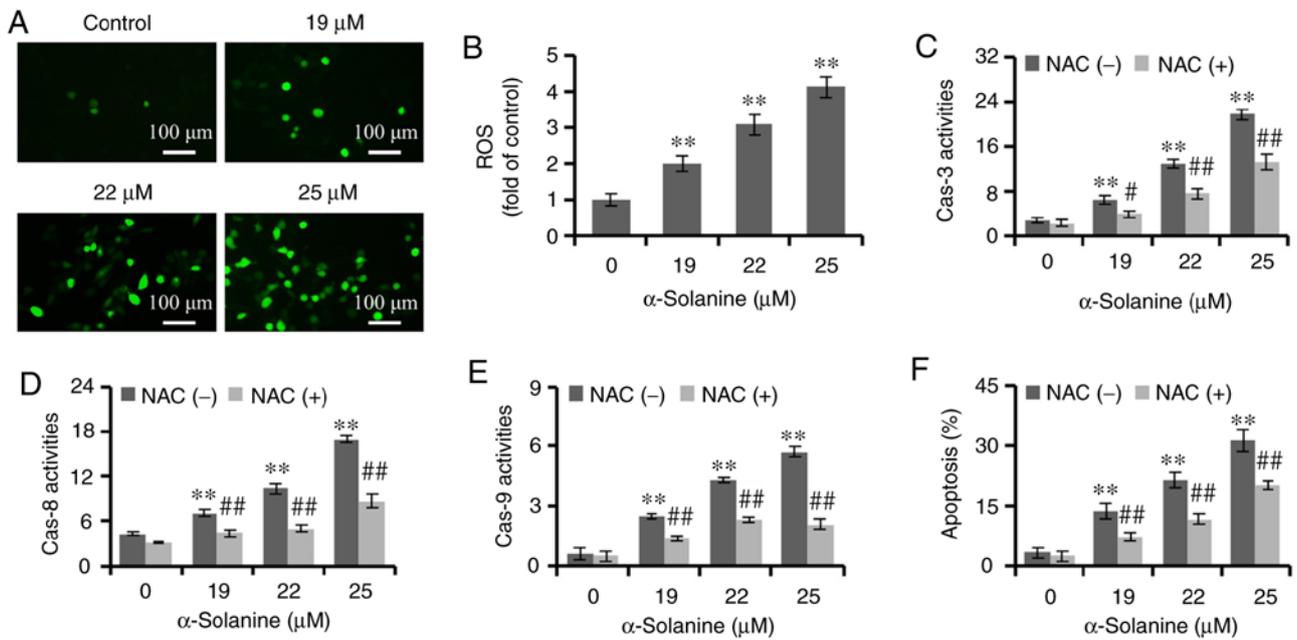
Figure 5. α-Solanine increases ROS generation in RKO cells. α-Solanine-treated RKO cells were stained with DCFH-DA, and (A) the green fluorescence was observed under a microscope (magnification, x200) and (B) detected by a plate reader. RKO cells were pre-treated with NAC, subjected to α-solanine treatment, followed by measurement of the activities of (C) caspase-3, (D) -8 and (E) -9, and (F) apoptosis detection. $^{**}$P<0.01 vs. control group; $^{#}$P<0.05, $^{##}$P<0.01 vs. α-solanine group. ROS, reactive oxygen species; NAC, N-acetyl-L-cysteine.
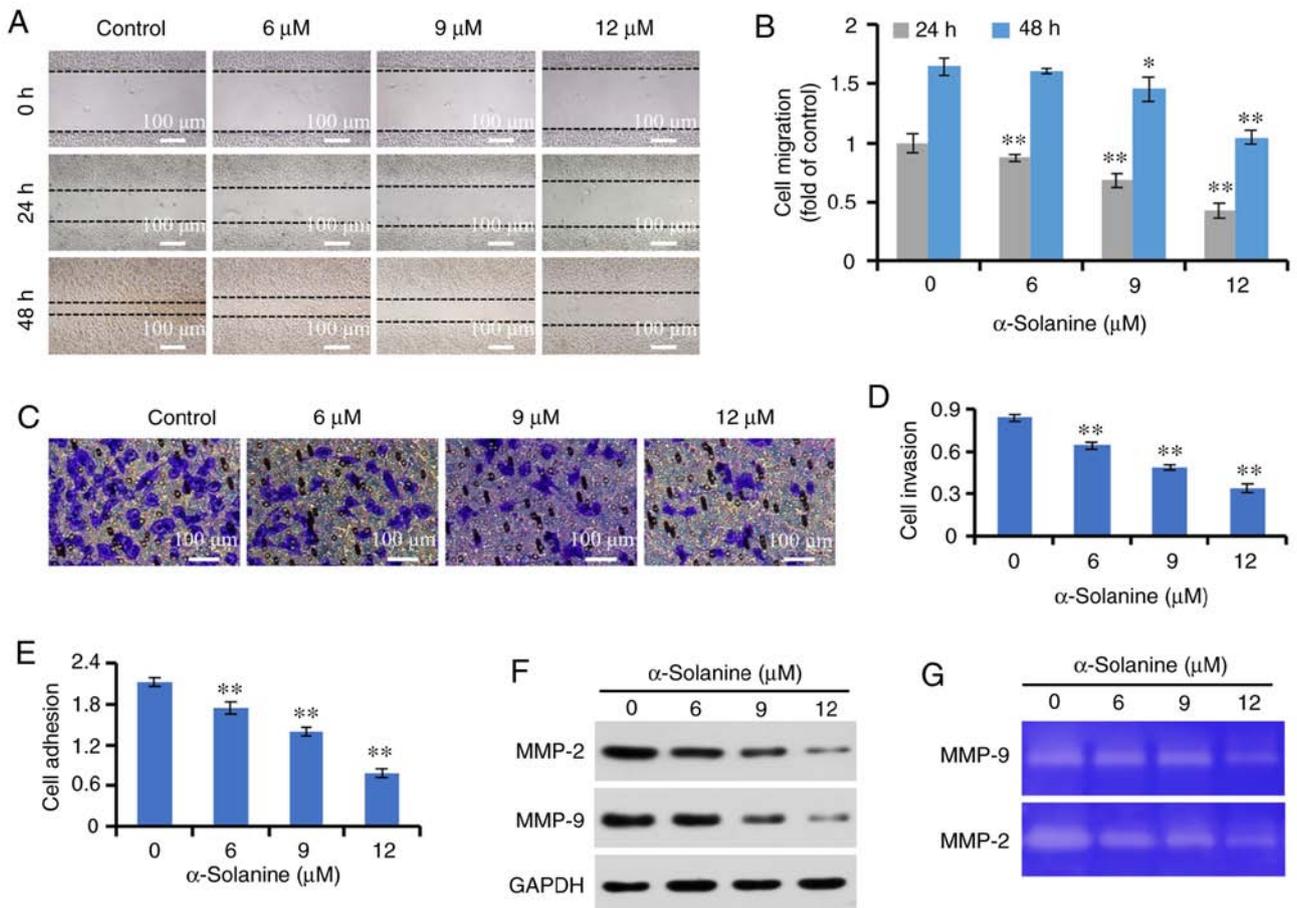


Figure 6. α-Solanine inhibits the metastatic potential of RKO cells. (A) The RKO cell layer was scratched by a sterile pipette tip and treated with α-solanine for 48 h; cell migration was observed under a microscope (magnification, x50), and (B) migration distances were expressed as fold-change over the control group. (C) Cell invasion was detected by Transwell assay, observed under a microscope (magnification, x200) and (D) measured by a plate reader (OD=560 nm). (E) Cell adhesion was detected by a commercial kit. (F) The expression of MMP-2 and MMP-9 was measured by western blotting. (G) The activities of MMP-2 and MMP-9 were detected by gelatin zymography assay. $^{*}$P<0.05, $^{**}$P<0.01 vs. control group. MMP, matrix metallopeptidase; OD, optical density.
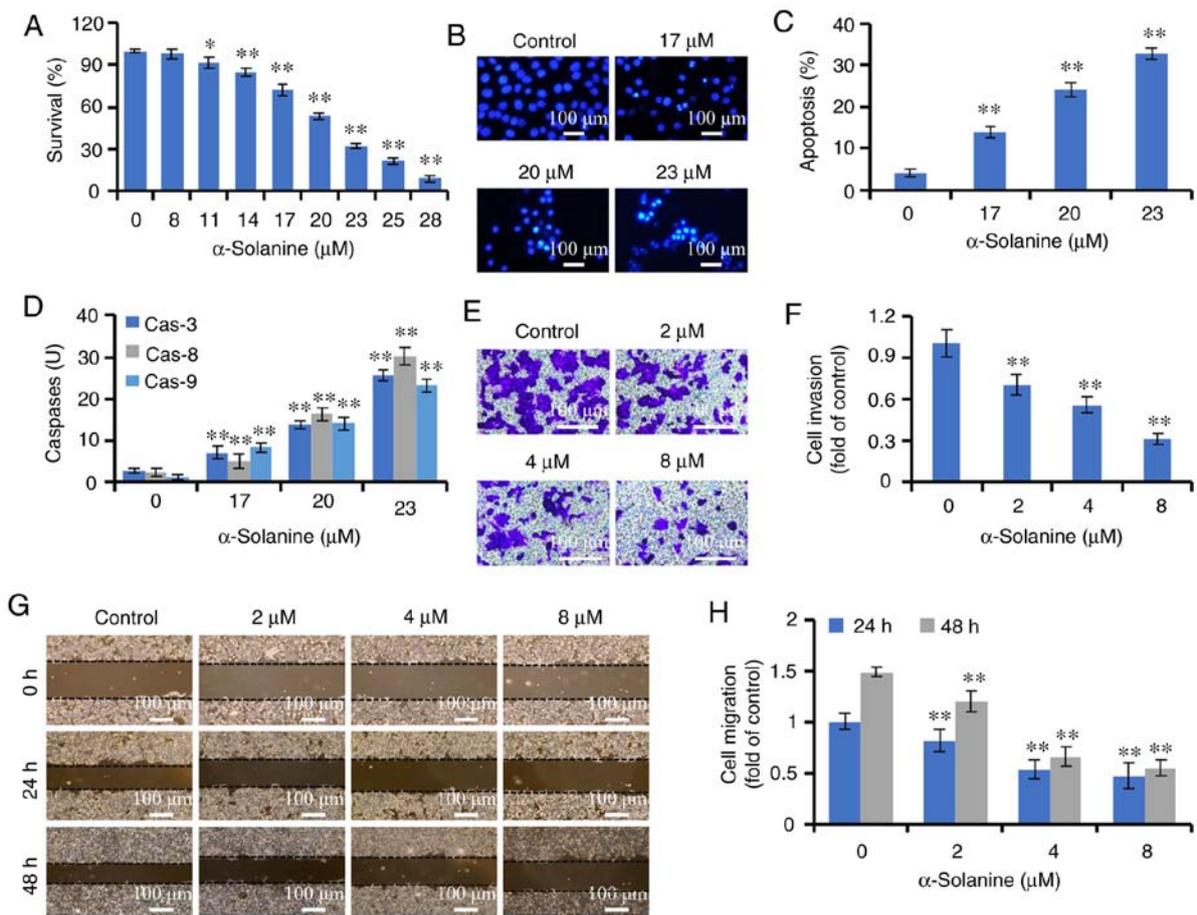
Figure 7. Effects of α-solanine on the growth and metastatic potential of HCT-116 cells. (A) HCT-116 cells were treated with 8-28 $\mu$M α-solanine for 48 h and subjected to Cell Counting Kit-8 assay. (B) HCT-116 cells were treated with α-solanine for 48 h, stained with Hoechst 33258, and observed under a microscope (magnification, x200). (C) HCT-116 cells were treated with α-solanine for 48 h, stained with AnnexinV-FITC/PI and analyzed by flow cytometry. (D) The activities of caspase-3, -8 and -9 were detected in α-solanine-treated HCT-116 cells. (E) Cell invasion was detected by Transwell assay, observed under a microscope (magnification, x100), and (F) expressed as fold of control. (G) Cell migration was measured by the scratch assay, observed under a microscope (magnification, x50) and (H) expressed as fold of control. $^{*}$P<0.05, $^{**}$P<0.01 vs. control group.

*α-Solanine suppresses the metastatic potential of RKO cells.* The scratch assay is a common method for detecting cell migration, which is widely used in various cell models (17,18). The results of the scratch assay revealed that the migration of RKO cells to the center of the scratch was reduced following treatment with low-dose α-solanine, which did not significantly affect cell proliferation, demonstrating that α-solanine inhibited the migration of RKO cells. Further studies revealed that low-dose α-solanine also inhibited the invasion and adhesion of RKO cells in a dose-dependent manner (P<0.01). In addition, low-dose α-solanine inhibited the expression and activities of MMP-2 and MMP-9 in RKO cells (Fig. 6).

*α-Solanine inhibits growth and metastasis of HCT-116 cells.* The effects of α-solanine on HCT-116 cells were also evaluated. As shown in Fig. 7, 11-28 $\mu$M α-solanine significantly inhibited the proliferation of HCT-116 cells in a dose-dependent manner (P<0.05). The IC$_{50}$ of α-solanine was 20.32 $\mu$M. α-Solanine induced apoptosis as indicated by Hoechst 33258 staining and flow cytometry analysis (P<0.01). α-Solanine also activated caspase-3, -8 and -9 (P<0.01). In addition, α-solanine inhibited the migration and invasion of HCT-116 cells (P<0.01).

*α-Solanine inhibits tumor growth.* To observed the effects of α-solanine on tumor growth, an RKO tumor was established in BALB/c nude mice. When the tumors became palpable, the mice were treated with α-solanine. As shown in Fig. 8, the tumors grew progressively in control group, whereas α-solanine significantly inhibited tumor growth as demonstrated by tumor volume and tumor weight (P<0.05). The expression of Ki-67, a proliferation marker, was detected by immunohistochemistry. α-Solanine inhibited Ki-67 expression, suggesting that α-solanine can inhibit cell proliferation *in vivo* (P<0.01). TUNEL assay was further used to identify apoptosis. Consistent with the *in vitro* observations, α-solanine induced apoptosis *in vivo* (P<0.01). The potential toxicity of α-solanine was also evaluated. Following treatment with α-solanine, no significant adverse consequences were observed, such as weight loss (Fig. 8C), ruffling of the fur, or changes in behavior and feeding (data not shown).

**Discussion**

Consistently with previous studies on other types of cancer (13-16), the present study demonstrated that α-solanine was able to inhibit the growth of colorectal cancer *in vitro*
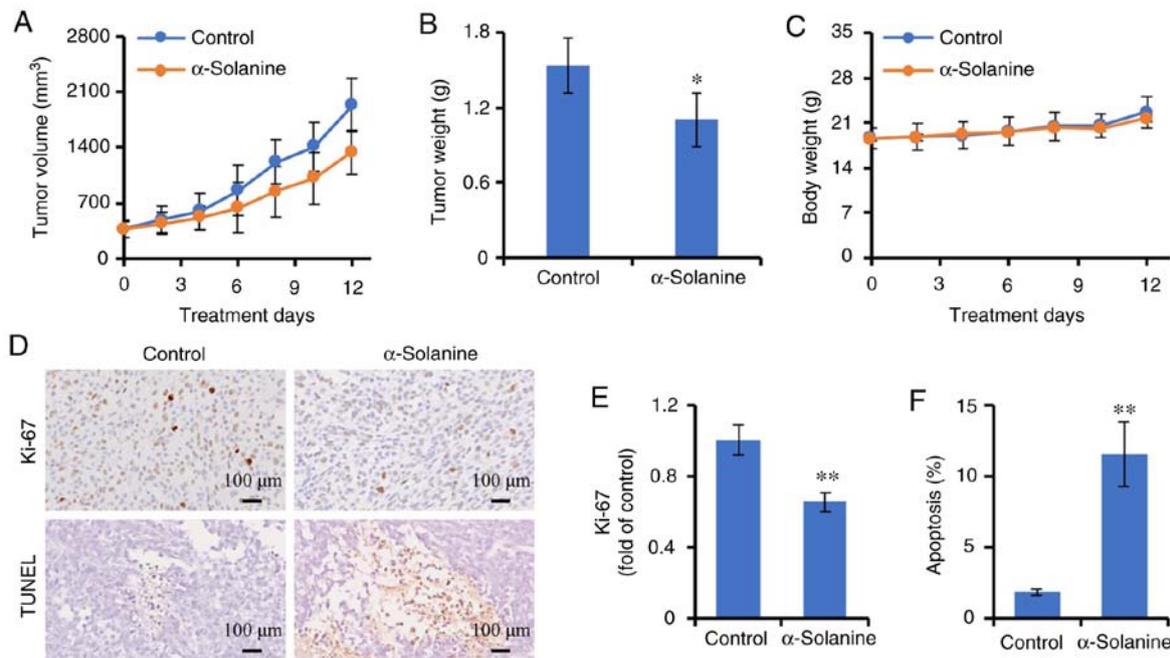
Figure 8. Effects of α-solanine on tumor growth. BALB/c nude mice were injected subcutaneously with RKO cells. When the tumors were palpable, the mice were randomized to receive treatment with α-solanine, or DMSO as a control. (A) Tumor volume. (B) Tumor weight. (C) Mouse body weight. (D) Ki-67 expression was detected by immunohistochemistry (upper panel), apoptosis was evaluated by the TUNEL assay (lower panel) and observed under a microscope (magnification, x200). (E) Ki-67 expression was quantified by Image-Pro Plus 6.0 software and expressed as fold of control. (F) Apoptosis was quantified by Image-Pro Plus 6.0 software. *P<0.05, **P<0.01 vs. control group.

and *in vivo*. Moreover, α-solanine arrested the cell cycle at the G0/G1 phase and reduced the number of cells in the S and G2/M phases. Additionally, α-solanine attenuated the expression of CCND1 and CDK4. CCND1 is a cell cycle regulatory protein that binds to CDK4, promotes phosphorylation of the retinoblastoma protein, activates transcription of target genes through E2F, e.g., cyclin E and CDK2, and also promotes cell cycle progression from the G1 to the S phase (23). The inhibition of CCND1 and CDK4 may lead to cell cycle arrest in colorectal cancer (24). Consequently, cell cycle arrest caused by decreased expression levels of CCND1 and CDK4 may be involved in the inhibition of proliferation by α-solanine.

Apoptosis is a cascade reaction mediated by caspases, as well as being an important mechanism of drug therapy for cancer (21,25). Apoptosis is mainly mediated by intrinsic and extrinsic pathways, activating caspase-3 through caspase-9 and caspase-8. Caspase-9 and caspase-8 are mediators of the intrinsic and extrinsic apoptotic pathways. In the present study, we observed that after treatment with α-solanine, colorectal cancer cells displayed an apoptotic morphology, with densely stained or fragmented nuclei. Annexin V-FITC/PI staining also demonstrated that α-solanine promoted apoptosis of colorectal cancer cells. The activities of caspase-3, -8 and -9 were simultaneously enhanced by α-solanine. These observations demonstrated that α-solanine induced apoptosis of colorectal cancer cells through the intrinsic and extrinsic pathways.

ROS are a normal product of cellular metabolism. However, high levels of ROS can promote cell apoptosis, and the underlying mechanism is associated with activation of caspases. Induction of ROS is crucial for tumor therapy (22,26). Natural products, such as oridonin, dioscin, ginsenoside Rh4 and bufalin, can promote apoptosis of colorectal cancer cells

through ROS (27-30). The present study demonstrated that α-solanine increased the level of ROS in RKO cells. NAC, as a ROS scavenger, antagonized the effects of α-solanine on activation of caspase-3, -8 and -9, and apoptosis induction, demonstrating that ROS may be involved in the α-solanine-induced apoptosis and the activation of caspases.

Tumor metastasis involves multiple biological processes, which include tumor cells shedding from the primary lesion, penetrating through the basement membrane, adhering to blood/lymphatic vessels, entering the blood/lymphatic circulation, adhering to the vascular endothelium, invading into target organs, and then proliferating to form metastatic foci. Tumor metastasis is closely associated with cell migration, invasion and adhesion (31,32). MMPs can degrade the ECM and participate in the process of tumor metastasis. MMP-2 and MMP-9 can promote the metastasis of colorectal cancer and exhibit a negative correlation with prognosis (33-36). Inhibition of MMP-2 and MMP-9 can inhibit the metastasis of colorectal cancer cells (37,38). The results of the present research indicate that α-solanine inhibited the migration, invasion and adhesion of colorectal cancer cells, accompanied by decreased expression and activity of MMP-2 and MMP-9, suggesting that the inhibitory effect of α-solanine on cell metastasis may be associated with MMP-2 and MMP-9.

In conclusion, the present study revealed that α-solanine inhibited cancer cell proliferation and tumor growth, reduced the expression levels of CCND1 and CDK4, arrested the cell cycle at the G0/G1 phase, increased the intracellular ROS level, activated caspase-3, -8 and -9, and induced apoptosis in colorectal cancer cells. Moreover, α-solanine also inhibited the migration, invasion and adhesion of colorectal cancer cells, which may be associated with the downregulation of MMP-2

and MMP-9. This constitutes new evidence supporting the application of α-solanine in the treatment of colorectal cancer. However, the lack of clinical data is the main limitation of the present study, and further research is required.

## Acknowledgements

Not applicable.

## Availability of data and materials

The datasets used and/or analyzed during the present study are available from the corresponding author on reasonable request.

## Authors' contributions

BH and KPS conceived and designed the study. XY, ML, LC, XP, ZJQ and HMA performed the experiments. XY analyzed the data and drafted the manuscript. BH revised the manuscript. All authors have read and approved the final manuscript.

## Ethics approval and consent to participate

All studies involving mice were approved by the Longhua Hospital Animal Care and Use Committee.

## Patient consent for publication

Not applicable.

## Competing interests

The authors declare that they have no competing interests.

## References

1. Bray F, Ferlay J, Soerjomataram I, Siegel RL, Torre LA and Jemal A: Global cancer statistics 2018: GLOBOCAN estimates of incidence and mortality worldwide for 36 cancers in 185 countries. CA Cancer J Clin 68: 394-424, 2018.
2. Ahmed S, Johnson K, Ahmed O and Iqbal N: Advances in the management of colorectal cancer: From biology to treatment. Int J Colorectal Dis 29: 1031-1042, 2014.
3. Rentsch M, Schiergens T, Khandoga A and Werner J: Surgery for colorectal cancer-trends, developments, and future perspectives. Visc Med 32: 184-191, 2016.
4. McQuade RM, Stojanovska V, Bornstein JC and Nurgali K: Colorectal cancer chemotherapy: The evolution of treatment and new approaches. Curr Med Chem 24: 1537-1557, 2017.
5. De Mello RA, Marques AM and Araújo A: Epidermal growth factor receptor and metastatic colorectal cancer: Insights into target therapies. World J Gastroenterol 19: 6315-6318, 2013.
6. Battaglin F, Puccini A, Intini R, Schirripa M, Ferro A, Bergamo F, Lonardi S, Zagonel V, Lenz HJ and Loupakis F: The role of tumor angiogenesis as a therapeutic target in colorectal cancer. Expert Rev Anticancer Ther 18: 251-266, 2018.
7. Passardi A, Canale M, Valgiusti M and Ulivi P: Immune checkpoints as a target for colorectal cancer treatment. Int J Mol Sci 18: pii: E1324, 2017.
8. Zhong LL, Chen HY, Cho WC, Meng XM and Tong Y: The efficacy of Chinese herbal medicine as an adjunctive therapy for colorectal cancer: A systematic review and meta-analysis. Complement Ther Med 20: 240-252, 2012.
9. Deng S, Hu B and An HM: Traditional Chinese medicinal syndromes and treatment in colorectal cancer. J Cancer Ther 3: 888-897, 2012.
10. Jain R, Sharma A, Gupta S, Sarethy IP and Gabrani R: *Solanum nigrum*: Current perspectives on therapeutic properties. Altern Med Rev 16: 78-85, 2011.
11. Hu B, An HM, Shen KP, Shi XF, Deng S and Wei MM: Effect of *Solanum nigrum* on human colon carcinoma RKO cells. Zhong Yao Cai 36: 958-961, 2013 (In Chinese).
12. Tai CJ, Wang CK, Tai CJ, Lin YF, Lin CS, Jian JY, Chang YJ and Chang CC: Aqueous extract of *Solanum nigrum* leaves induces autophagy and enhances cytotoxicity of cisplatin, doxorubicin, docetaxel, and 5-fluorouracil in human colorectal carcinoma cells. Evid Based Complement Alternat Med 2013: 514719, 2013.
13. Mohsenikia M, Alizadeh AM, Khodayari S, Khodayari H, Kouhpayeh SA, Karimi A, Zamani M, Azizian S and Mohagheghi MA: The protective and therapeutic effects of alpha-solanine on mice breast cancer. Eur J Pharmacol 718: 1-9, 2013.
14. Lv C, Kong H, Dong G, Liu L, Tong K, Sun H, Chen B, Zhang C and Zhou M: Antitumor efficacy of α-solanine against pancreatic cancer in vitro and in vivo. PLoS One 9: e87868, 2014.
15. Shen KH, Liao AC, Hung JH, Lee WJ, Hu KC, Lin PT, Liao RF and Chen PS: α-Solanine inhibits invasion of human prostate cancer cell by suppressing epithelial-mesenchymal transition and MMPs expression. Molecules 19: 11896-11914, 2014.
16. Meng XQ, Zhang W, Zhang F, Yin SY, Xie HY, Zhou L and Zheng SS: Solanine-induced reactive oxygen species inhibit the growth of human hepatocellular carcinoma HepG2 cells. Oncol Lett 11: 2145-2151, 2016.
17. Yarrow JC, Perlman ZE, Westwood NJ and Mitchison TJ: A high-throughput cell migration assay using scratch wound healing, a comparison of image-based readout methods. BMC Biotechnol 4: 21, 2004.
18. Liang CC, Park AY and Guan JL: In vitro scratch assay: A convenient and inexpensive method for analysis of cell migration in vitro. Nat Protoc 2: 329-333, 2007.
19. Hu B, An HM, Yan X, Zheng JL, Huang XW and Li M: Traditional Chinese medicine formulation Yanggan Jiedu Sanjie inhibits TGF-β1-induced epithelial-mesenchymal transition and metastatic potential in human hepatocarcinoma Bel-7402 cells. BMC Complement Altern Med 19: 67, 2019.
20. Hu B, An HM, Wang SS, Zheng JL, Yan X, Huang XW and Tian JH: Teng-Long-Bu-Zhong-Tang induces p21-dependent cell senescence in colorectal carcinoma LS174T cells via histone acetylation. J Exp Pharmacol 9: 67-72, 2017.
21. Kaczanowski S: Apoptosis: Its origin, history, maintenance and the medical implications for cancer and aging. Phys Biol 13: 031001, 2016.
22. Redza-Dutordoir M and Averill-Bates DA: Activation of apoptosis signalling pathways by reactive oxygen species. Biochim Biophys Acta 1863: 2977-2992, 2016.
23. Asghar U, Witkiewicz AK, Turner NC and Knudsen ES: The history and future of targeting cyclin-dependent kinases in cancer therapy. Nat Rev Drug Discov 14: 130-146, 2015.
24. Chen MJ, Cheng AC, Lee MF and Hsu YC: Simvastatin induces G1 arrest by up-regulating GSK3β and down-regulating CDK4/cyclin D1 and CDK2/cyclin E1 in human primary colorectal cancer cells. J Cell Physiol 233: 4618-4625, 2018.
25. Goldar S, Khaniani MS, Derakhshan SM and Baradaran B: Molecular mechanisms of apoptosis and roles in cancer development and treatment. Asian Pac J Cancer Prev 16: 2129-2144, 2015.
26. Zou Z, Chang H, Li H and Wang S: Induction of reactive oxygen species: An emerging approach for cancer therapy. Apoptosis 22: 1321-1335, 2017.
27. Oh HN, Seo JH, Lee MH, Yoon G, Cho SS, Liu K, Choi H, Oh KB, Cho YS, Kim H, *et al*: Oridonin induces apoptosis in oral squamous cell carcinoma probably through the generation of reactive oxygen species and the p38/JNK MAPK pathway. Int J Oncol: Mar 16, 2018 (Epub ahead of print).

28. Li S, Cheng B, Hou L, Huang L, Cui Y, Xu D, Shen X and Li S: Dioscin inhibits colon cancer cells' growth by reactive oxygen species-mediated mitochondrial dysfunction and p38 and JNK pathways. Anticancer Drugs 29: 234-242, 2018.

29. Wu Q, Deng J, Fan D, Duan Z, Zhu C, Fu R and Wang S: Ginsenoside Rh4 induces apoptosis and autophagic cell death through activation of the ROS/JNK/p53 pathway in colorectal cancer cells. Biochem Pharmacol 148: 64-74, 2018.

30. Wu D, Zhou WY, Lin XT, Fang L and Xie CM: Bufalin induces apoptosis via mitochondrial ROS-mediated caspase-3 activation in HCT-116 and SW620 human colon cancer cells. Drug Chem Toxicol 42: 444-450, 2019.

31. Valastyan S and Weinberg RA: Tumor metastasis: Molecular insights and evolving paradigms. Cell 147: 275-292, 2011.

32. Guan X: Cancer metastases: Challenges and opportunities. Acta Pharm Sin B 5: 402-418, 2015.

33. Dong W, Li H, Zhang Y, Yang H, Guo M, Li L and Liu T: Matrix metalloproteinase 2 promotes cell growth and invasion in colorectal cancer. Acta Biochim Biophys Sin (Shanghai) 43: 840-848, 2011.

34. Shi M, Yu B, Gao H, Mu J and Ji C: Matrix metalloproteinase 2 overexpression and prognosis in colorectal cancer: A meta-analysis. Mol Biol Rep 40: 617-623, 2013.

35. Mook OR, Frederiks WM and Van Noorden CJ: The role of gelatinases in colorectal cancer progression and metastasis. Biochim Biophys Acta 1705: 69-89, 2004.

36. Yang B, Tang F, Zhang B, Zhao Y, Feng J and Rao Z: Matrix metalloproteinase-9 overexpression is closely related to poor prognosis in patients with colon cancer. World J Surg Oncol 12: 24, 2014.

37. Oba K, Konno H, Tanaka T, Baba M, Kamiya K, Ohta M, Kaneko T, Shouji T, Igarashi A and Nakamura S: Prevention of liver metastasis of human colon cancer by selective matrix metalloproteinase inhibitor MMI-166. Cancer Lett 175: 45-51, 2002.

38. Kang JH, Han IH, Sung MK, Yoo H, Kim YG, Kim JS, Kawada T and Yu R: Soybean saponin inhibits tumor cell metastasis by modulating expressions of MMP-2, MMP-9 and TIMP-2. Cancer Lett 261: 84-92, 2008.